Journal of Alloys and Compounds 509 (2011) 4649–4652

Contents lists available at ScienceDirect

Journal of Alloys and Compounds

journal homepage: www.elsevier.com/locate/jallcom

Luminescence properties of $Ca_{10}K(PO_4)_7$:RE^{3+} (RE = Ce, Tb, Dy, Tm and Sm) under vacuum ultraviolet excitation

Jia Zhang, Yuhua Wang*, Yan Wen, Feng Zhang, Bitao Liu

Department of Material Science, School of Physical Science and Technology, Lanzhou University, Lanzhou 730000, PR China

ARTICLE INFO

Article history:
Received 20 September 2010
Received in revised form 9 January 2011
Accepted 19 January 2011
Available online 26 January 2011

Keywords:
Optical properties
Luminescence
Rare-earth

ABSTRACT

A series of RE^{3+} (RE = Ce, Tb, Dy, Tm and Sm) activated $Ca_{10}K(PO_4)_7$ were synthesized by conventional state reaction and their photoluminescence properties under vacuum ultraviolet excitation were investigated. The $PO_4{}^{3-}$ absorption lies within the range from 125 to 180 nm in all the excitation spectra of $Ca_{10}K(PO_4)_7$:RE^{3+}. The first f–d transition of Ce^{3+} is observed at 316 nm, and the Ce^{3+} emission is located at about 350 nm. Both the first spin-allowed and spin-forbidden f–d transitions of Tb^{3+} are situated at 232 and 263 nm, respectively. The emission spectrum of $Ca_{10}K(PO_4)_7$:Tb^{3+} exhibits typical Tb^{3+} emissions with the predominant peak at 544 nm. The O^{2-}–Dy^{3+} charge transition band was calculated and identified around 173 nm, the CIE chromaticity coordinates of Dy^{3+} were calculated to be 0.364 and 0.392. The $Ca_{10}K(PO_4)_7$:Tm^{3+} demonstrates the strongest excitation at about 182 nm assigned to O^{2-}–Tm^{3+}, and gives the predominant emission at 453 nm. The $^4G_{5/2}$–$^6H_{7/2}$ transition of Sm^{3+} at 601 nm is the most intensive in the emission spectrum.

1. Introduction

In the past few years, the luminescence spectroscopy of rare-earth (RE) ions in the vacuum ultraviolet (VUV) spectral range has attracted a considerable attention [1,2] due to the main reasons as follow: firstly, it is urgent to explore new efficient VUV-excited phosphors for Hg-free fluorescent lamps and plasma display panels (PDPs); secondly, it is necessary to carry out researches on the theory of luminescence to understand the luminescence mechanism of RE-doped phosphors in the VUV region. As is known, the plasma of xenon containing noble gas mixture, whose emission consists of the Xe resonance emission line (147 nm) and/or the Xe_2 molecular emission band (172 nm), provides the excitation resource in PDPs or Hg-free lamps [3–5]. And the luminescence properties of phosphors directly influence the performances of PDPs and Hg-free lamps. Recently, $BaMgAl_{10}O_{17}$:Eu^{2+} (BAM), Zn_2SiO_4:Mn^{2+} and (Y, Gd)BO_3:Eu^{3+} have been commercially used as blue, green and red phosphors for PDPs, respectively. Among these phosphors, BAM is easily degraded by a thermal treatment in the presence of oxygen during panel fabrication and VUV damage during panel operation [6]; the decay time of the Zn_2SiO_4:Mn^{2+} phosphor is too long resulting in that one image could be superimposed on another [7]; the red phosphor exhibits a poor color purity, because the intensity of the orange emission is higher than that of the red one [8]. Hence, new phosphors with good characteristics such as intensive emission upon 147/172 nm excitation are imperatively needed.

Recent studies [9–11] have found that RE^{3+}-activated phosphates could exhibit excellent luminescence properties due to the absorption of $PO_4{}^{3-}$ in VUV region [12]. It was reported that $Ca_{10}K(PO_4)_7$ (CKP) compound is isostructural to β-$Ca_3(PO_4)_2$, which have a polar whitlockite-type crystal structure [13]. And many kinds of materials with different cations substituting in the initial β-$Ca_3(PO_4)_2$ have served as the base for the crystallochemical design of compounds with ferroelectric, nonlinear-optical and ion-conductive properties [14,15]. To the best of our knowledge, the ultraviolet (UV) optical properties of CKP:Eu^{2+}, Tb^{3+} have been investigated [16]. However, the photoluminescence (PL) properties of RE^{3+}-doped CKP in VUV region have not been reported. In this paper, to explore new VUV phosphors and carry out basic research, we synthesized the CKP:RE^{3+} (RE = Ce, Tb, Dy, Tm and Sm) samples and investigated their VUV spectroscopic properties.

2. Experimental

RE^{3+}-doped CKP (RE = Ce, Tb, Dy, Tm and Sm) were synthesized by conventional solid-state reaction. The starting materials included $CaCO_3$ (99%), $NH_4H_2PO_4$ (99%), K_2CO_3 (99%), CeO_2 (99.99%), Tb_4O_7 (99.99%), Dy_2O_3 (99.99%), Tm_2O_3 (99.99%) and Sm_2O_3 (99.99%). When RE oxides were doped into the CKP matrix, the equally K_2CO_3 serves as a charge compensation reagent. Stoichiometric amounts of the starting reagents were thoroughly mixed and ground together by an agate mortar. An excess (5%) of $NH_4H_2PO_4$ was used to compensate for the evaporation at a high temperature. The mixture was pre-fired in air at 600 °C for 3 h, reground, then calcined in air (for Dy, Tm and Sm doped samples) or in a reduction atmosphere (N_2:H_2 = 95:5, for Ce and Tb doped samples) at 1210 °C for 7 h. The concentrations of RE^{3+} (RE = Ce, Tb, Dy, Tm and Sm) activators are 2 mol% of Ca^{2+}.

---

* Corresponding author. Tel.: +86 931 8912772; fax: +86 931 8913554.
E-mail address: wyh@lzu.edu.cn (Y. Wang).

0925-8388/$ – see front matter © 2011 Elsevier B.V. All rights reserved.
doi:10.1016/j.jallcom.2011.01.125

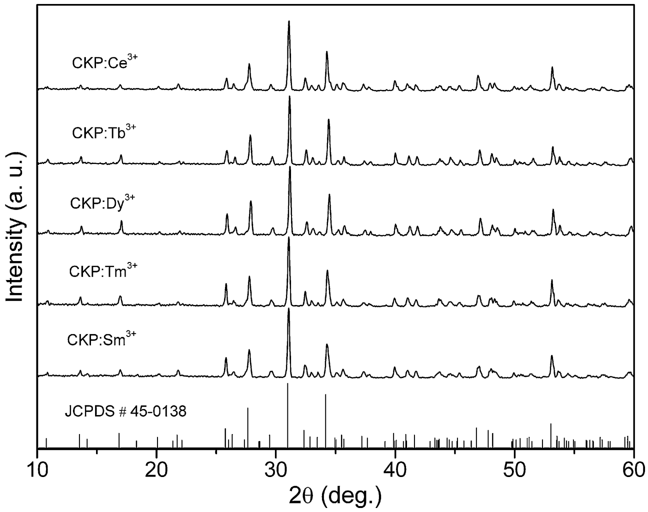

Fig. 1. XRD patterns of CKP:RE^{3+} (RE = Ce, Tb, Dy, Tm and Sm).

The phase purity was determined using a Rigaku D/MAX-2400 powder X-ray diffractometer (XRD) with Cu Kα radiation (λ = 1.54178 Å) operating at 40 kV and 20 mA. The photoluminescence (PL) and photoluminescence excitation (PLE) spectra were measured by a FLS920T spectrophotometer equipped with VM504 vacuum monochromator, and the PLE spectra were corrected by the sodium salicylate at the same measurement conditions. All the spectra measurements were performed at room temperature.

3. Results and discussion

3.1. XRD analysis

The XRD studies were performed on CKP:RE^{3+} (RE = Ce, Tb, Dy, Tm and Sm) as shown in Fig. 1. The pattern shows that all of the reflected peaks are identified to CKP host lattice which crystallizes in hexagonal structure (JCPDS-45-0138), indicating the single phase samples can be successfully obtained by solid-state reaction when a small quantity of RE^{3+} was doped into the CKP matrix.

3.2. Photoluminescence properties

3.2.1. Ce^{3+}-doped CKP

Fig. 2 presents both the excitation excited at 147 nm and the emission spectra monitored at 350 nm of CKP:Ce^{3+}, respectively. In Ref. [17], Saito et al. have calculated the energy levels of tetrahedral $PO_4{}^{3-}$ molecule using the extended Hückel method. According to their results, the lowest intramolecular transition of $2t_2 \rightarrow 2a,3t_2$ was found to exist at 7–10 eV (124–177 nm). And in many phosphates, the absorption position of the $PO_4{}^{3-}$ has been reported at this range [9–11,18]. Therefore, the excitation band from 130 to 180 nm in Fig. 2 could attributed to the $PO_4{}^{3-}$ absorption of the host. And the remaining excitation band from 180 to 350 nm could be attributed to the f–d transition of Ce^{3+} due to its broad and strong characteristics, from which it can be seen the first f–d transition of Ce^{3+} in CKP:Ce^{3+} is located at 316 nm. Upon 147 nm excitation, the emission spectrum exhibits a broad emission band located at about 350 nm, which could be assigned to the d–f transition of Ce^{3+}.

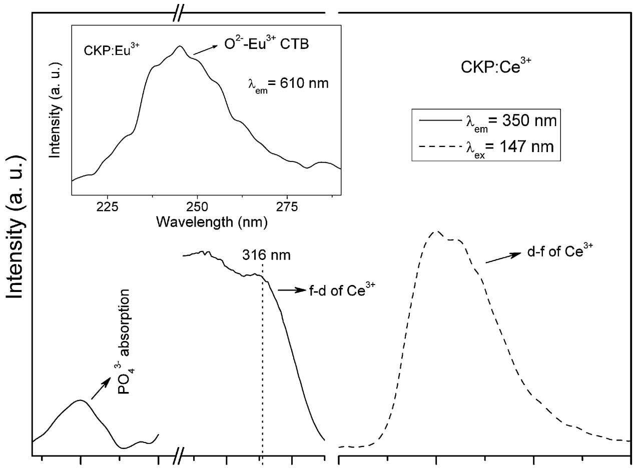

Fig. 2. Excitation and emission spectra of CKP:Ce^{3+}.

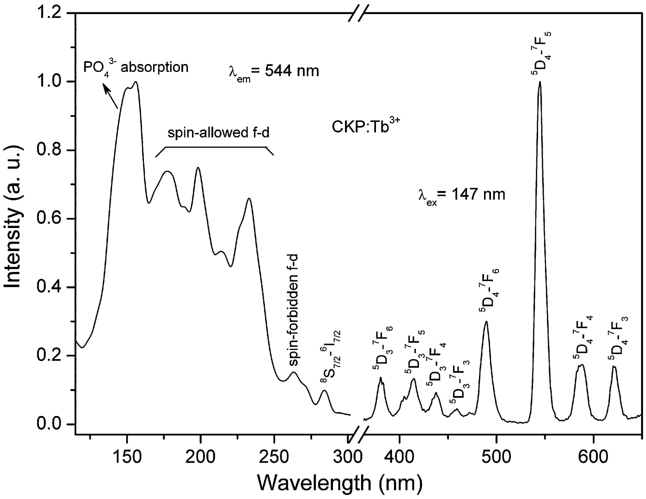

Fig. 3. Excitation and emission spectra of CKP:Tb^{3+}.

3.2.2. Tb^{3+}-doped CKP

Both the excitation and emission spectra of CKP:Ce^{3+} are shown in Fig. 3. Upon 147 nm excitation, the emission spectrum consists of a group of typical $^5D_{3,4} \rightarrow {}^7F_J$ (J = 3–6) transitions of Tb^{3+}, among which the $^5D_4 \rightarrow {}^7F_5$ transition at 544 nm is predominant. On the other hand, the $^5D_3 \rightarrow {}^7F_J$ (J = 3–6) transitions of Tb^{3+} can be observed obviously, this is due to that the spectral energy distribution of Tb^{3+} emission depends strongly on Tb^{3+} concentration [11]. At a low concentration of Tb^{3+}, the emissions from $^5D_3$ to ^7F_J levels can be observed easily; with an increase of Tb^{3+} concentration, the emissions from $^5D_3$ to ^7F_J levels are quenched gradually by the cross relaxation process, as described in formula (1).

$$Tb^3({}^5D_3) + Tb^3({}^7F_6) \rightarrow Tb^3({}^5D_4) + Tb^3({}^7F_0) \qquad (1)$$

From the excitation spectrum monitored at 544 nm, it can be seen that the CKP:Tb^{3+} phosphor could be efficiently excited by 147 nm, and the excitation band between 125 and 165 nm could be attributed to the host absorption according to the analysis above. For Tb^{3+} ions, when one electron is promoted to 5d shell, it gives rise to two $4f^75d^1$ excitation states: the high-spin state with ^9D_J configurations and the low-spin state with ^7D_J configurations. Correspondingly, the 4f–4f5d transitions include the $^7F_J \rightarrow {}^9D_J$ and $^7F_J \rightarrow {}^7D_J$ transitions which are spin-forbidden (SF) and spin-allowed (SA), respectively. In addition, it is well known that the relative energy of the first f–d transition for different RE^{3+} ions is strongly dependent of host and the defined crystal show somewhat lower energies compared with the 5d orbital energy of the free RE^{3+} ions [19]. Dorenbos [2] proposed that crystal-field decrease $D(\mathrm{Ln}, A)$ for the energy of the $4f^{n-1}5d$ levels of a lanthanide ion in compounds A relative to the same level energies in the free

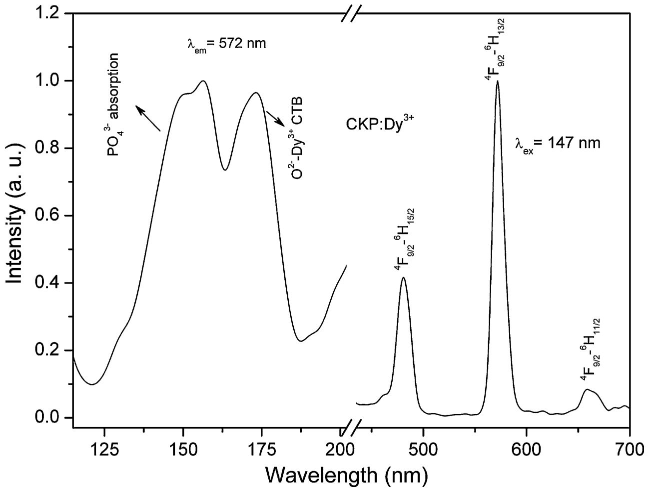

Fig. 4. Excitation and emission spectra of CKP:Dy^{3+}.

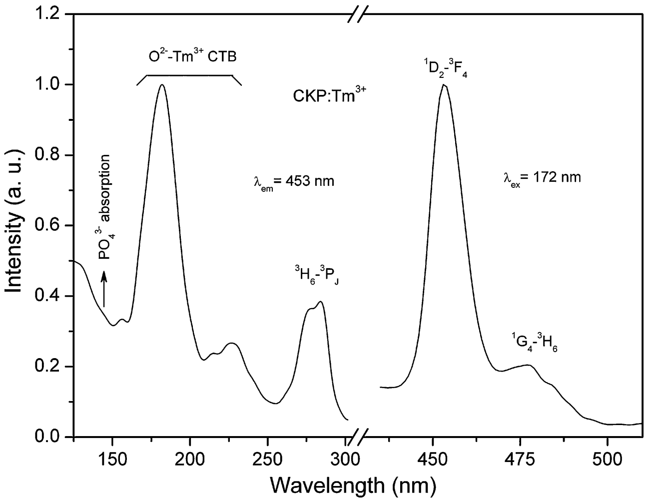

Fig. 5. Excitation and emission spectra of CKP:Tm^{3+}.

ion, i.e.

$$E(\mathrm{Ln}, A) = 49,340\,\mathrm{cm}^{-1} - D(A) + \Delta E^{\mathrm{Ln,Ce}} \tag{2}$$

is almost independent of the nature of lanthanide ion doped. Here, $E(\mathrm{Ln}, A)$ is the f–d energy difference of the lanthanide ions Ln^{3+} doped in compound A, $D(A)$ is the energy that the lowest 4f–5d excitation band is lowered relative to that of free Ce^{3+} ion, and $\Delta E^{\mathrm{Ln,Ce}}$ is the energy shift between the lowest 4f–5d excitation band of Ln^{3+} with respect to that of Ce^{3+}. The first f–d transition of Ce^{3+} in CKP:Ce^{3+} is observed at 316 nm as shown in Fig. 2, so the $D(A)$ could be calculated to 17,694 cm^{-1}. Both the 5d levels of free Tb^{3+} for the SF and SA f–d transitions are reported to be 62,500 and 56,200 cm^{-1} [2], respectively. By Eq. (2), we can obtain the first SF and SA f–d transitions of Tb^{3+} in CKP:Tb^{3+} to be 44,806 cm^{-1} (223 nm) and 38,506 cm^{-1} (260 nm), respectively. Correspondingly, the strong excitation band around 232 nm could be attributed to the first SA f–d transitions of Tb^{3+} and the weak excitation band around 263 nm could be assigned to the SF f–d transitions of Tb^{3+}.

3.2.3. Dy^{3+}-doped CKP

It is well known that the color of the Dy^{3+} luminescence is close to white due to the blue emission (about 480 nm) and the yellow emission (about 570 nm). Both the excitation and emission spectra of CKP:Dy^{3+} are represented in Fig. 4. Upon 147 nm excitation, the CKP:Dy^{3+} gives three emission peaks at 481, 572 and 659 nm, ascribed to the $^4F_{9/2}$–$^6H_{15/2}$, $^4F_{9/2}$–$^6H_{13/2}$ and $^4F_{9/2}$–$^6H_{11/2}$ transitions, respectively. And the intensity of $^4F_{9/2}$–$^6H_{13/2}$ emission is much stronger than that of $^4F_{9/2}$–$^6H_{15/2}$ emission. As we know, the $^4F_{9/2}$–$^6H_{13/2}$ transition belongs to the hypersensitive transition with $\Delta J = 2$, which is strongly influenced by the outside environment of Dy^{3+} and is allowed only at low symmetries with no inversion centre; the $^4F_{9/2}$–$^6H_{15/2}$ transition is magnetically allowed, which hardly varies with the crystal field strength around the Dy^{3+} [10,20]. The CKP is isostructural to β-$Ca_3(PO_4)_2$, which has no inversion centre in this structure [13,21], so the emission spectra of CKP:Dy^{3+} demonstrate a large ratio of the yellow emission intensity to the blue one. The Commission International del'Eclairage (CIE) chromaticity coordinates of CKP:Dy^{3+} are calculated using the emission spectrum dates to be 0.364, 0.392, indicating a near-white emission. The excitation spectrum of CKP:Dy^{3+} monitored at 572 nm demonstrates two strong excitation bands in VUV region. As discussed above, the former excitation band from 125 to 163 nm could be attributed to the PO_4^{3-} absorption. And the attribution of the latter one needs discussing in detailed. Generally, the charge transfer band (CTB) is usually of strong and broad character, and the CTB positions of other RE^{3+} ions can be predicted once that of any one RE^{3+} ion such as Eu^{3+} is known with the help of an empirical formula given by Jørgensen [22]:

$$E_{\mathrm{ct}}(\mathrm{cm}^{-1}) = [\chi_{\mathrm{opt}}(X) - \chi_{\mathrm{uncorr}}(M)] \times 30,000\,\mathrm{cm}^{-1} \tag{3}$$

where E_{ct} (cm^{-1}) gives the position of the CTB. χ_{opt} (X) is the optical electro-negativity of the ligand ion (viz. oxygen in the present system). χ_{uncorr} (M) is the uncorrected optical electro-negativity of the central metal ion. The UV excitation spectrum of CKP:Eu^{3+} is presented in the inset of Fig. 2, the broad band around about 245 nm could be attributed to the O^{2-}–Eu^{3+} CTB. According to Ref. [23], the optical electro-negativity of Eu^{3+} and Dy^{3+} is 1.74 and 1.21 eV, respectively. Therefore, the CTB energy of Dy^{3+} in CKP:Dy^{3+} can be calculated to 56,716 cm^{-1} (viz. 176 nm). In this case, the latter excitation band located at 173 nm in Fig. 4 could be ascribed to the O^{2-}–Dy^{3+} CTB.

3.2.4. Tm^{3+}-doped CKP

Fig. 5 shows both the excitation and emission spectra of CKP:Tm^{3+}. From the excitation spectrum monitored at 453 nm, it can be seen that the CKP:Tm^{3+} exhibits a weak host absorption, but a relatively strong excitation band centred at 182 nm is observed obviously, which could be assigned to the O^{2-}–Tm^{3+} CTB according to the calculated result by Eq. (3). In the UV region, there are a group of excitation peaks existing between 260 and 300 nm that can be assigned to the $^3H_6$–^3P_J (J = 2, 1, 0) transitions [24]. Upon 172 nm excitation, the predominant emission peak is located at 453 nm, attributed to the $^1D_2$–$^3F_4$ transition of Tm^{3+} [24]. Besides, there is a weak emission at about 478 nm, and it could be ascribed to the $^1G_4$–$^3H_6$ transition of Tm^{3+} [24]. As a whole, the brightness of CKP:Tm^{3+} is somewhat low. That is because for Tm^{3+} with complex levels in $4f^{12}$ configuration, the electron–phonon coupling plays an important role in the relaxation process of Tm^{3+}, which will lower the blue emission [10].

3.2.5. Sm^{3+}-doped CKP

The excitation spectrum by monitoring at 601 nm and the emission spectrum upon 147 nm excitation are both shown in Fig. 6. Similarly, the excitation band from 125 to 163 nm could be associated to the host absorption. By Eq. (2), the first f–d transition position of Sm^{3+} is calculated to 172 nm that is very close to the position of the excitation peak centred at 174 nm, so the band from 163 to 195 nm could be attributed to the f–d transition of Tm^{3+}. In Ref. [18], the O^{2-}–Sm^{3+} CTB in the $Ba_3(PO_4)_2$:Sm^{3+} phosphor has been reported at 223 nm. And considering the broad

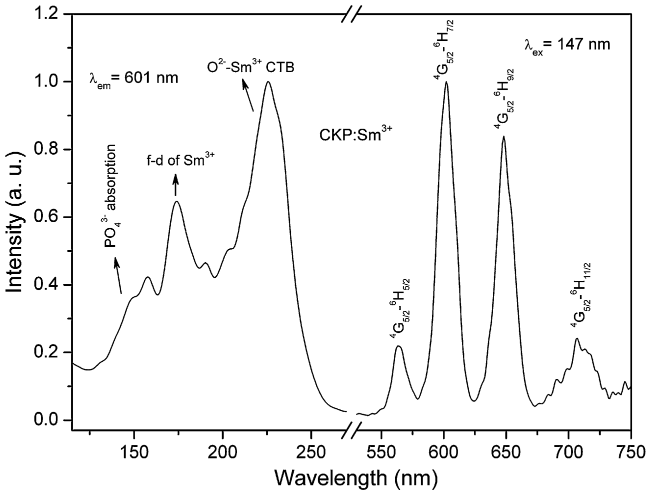

Fig. 6. Excitation and emission spectra of CKP:Sm^{3+}.

and strong character of CTB, the intensive excitation band around 225 nm in Fig. 6 could be ascribed to the O^{2-}–Sm^{3+} CTB. The emission spectrum demonstrates the typical emissions of Sm^{3+}, and the predominant emission peak is located at 601 nm ascribed to the $^4G_{5/2}$–$^6H_{7/2}$ transition. The other three relatively weak peaks at 563, 648 and 707 nm are attributed to the $^4G_{5/2}$–$^6H_{5/2}$, $^4G_{5/2}$–$^6H_{9/2}$ and $^4G_{5/2}$–$^6H_{11/2}$, respectively [25].

4. Conclusions

In conclusion, we prepared Ce, Tb, Dy, Tm and Sm doped CKP samples by solid-state reaction, and studied their PL and PLE properties in VUV region. The host absorption in all of these phosphors is located between 125 and 180 nm. The first f–d transition of Ce^{3+} is observed at 316 nm. Both the CKP:Tb^{3+} and CKP:Dy^{3+} exhibit intensive excitation in VUV region, and their predominant emissions are at 544 and 572 nm, respectively. Under 172 nm excitation, the CKP:Tm^{3+} gives the strongest emission at 453 nm. Upon 147 nm, four emission peaks are observed at 563, 601, 648 and 707 nm at the range from 550 to 750 nm for CKP:Sm^{3+}. To sum up, the investigations on CKP:RE^{3+} will enrich the RE-doped luminescence materials excited by VUV light and contribute to the applications for PDPs and Hg-free lamps.

Acknowledgments

This work was supported by the National Science Foundation for Distinguished Young Scholars (No. 50925206), the National Natural Science Foundation of China (No. 10874061) and the Research Fund for the Doctoral Program of Higher Education (No. 200807300010).

References

[1] R.T. Wegh, H. Donker, A. Meijerink, Phys. Rev. B 56 (1997) 13841–13848.
[2] P. Dorenbos, J. Lumin. 91 (2000) 91–106.
[3] Z.-J. Zhang, J.-L. Yuan, X.-J. Wang, D.-B. Xiong, H.-H. Chen, J.-T. Zhao, Y.-B. Fu, Z.-M. Qi, G.-B. Zhang, C.-S. Shi, J. Phys. D: Appl. Phys. 40 (2007) 1910–1914.
[4] H.B. Liang, Y. Tao, J.H. Xu, H. He, H. Wu, W.X. Chen, S.B. Wang, Q. Su, J. Solid State Chem. 177 (2004) 901–908.
[5] Z.Y. Zhang, Y.H. Wang, J.C. Zhang, Mater. Lett. 62 (2008) 846–848.
[6] K.Y. Jung, K.H. Han, Y.C. Kang, H.-K. Jung, Mater. Chem. Phys. 98 (2006) 330–336.
[7] H.S. Yoo, W.B. Im, J.H. Kang, D.Y. Jeon, Opt. Mater. 31 (2008) 131–135.
[8] X.L. Gao, Y.H. Wang, D. Wang, B.T. Liu, J. Lumin. 129 (2009) 840–843.
[9] D. Wang, Y.H. Wang, Mater. Sci. Eng. B 133 (2006) 218–221.
[10] Z.-J. Zhang, J.-L. Yuan, H.-H. Chen, X.-X. Yang, J.-T. Zhao, G.-B. Zhang, C.-S. Shi, Solid State Sci. 11 (2009) 549–555.
[11] W.H. Di, X.J. Wang, B.J. Chen, H.S. Lai, X.X. Zhao, Opt. Mater. 27 (2005) 1386–1390.
[12] K.C. Mishra, I. Osterloh, H. Anton, B. Hannebauer, P.C. Schmidt, K.H. Johnson, J. Lumin. 72–74 (1997) 144–145.
[13] B. Dickens, L.W. Schroeder, W.E. Brown, J. Solid State Chem. 10 (1974) 232–248.
[14] A.V. Teterskii, S.Y. Stefanovich, B.I. Lazoryak, D.A. Rusakov, Russ. J. Inorg. Chem. 52 (2007) 308–314.
[15] Y.L. Huang, H.Y. Ding, K. Jang, E. Cho, H.S. Lee, M. Jayasimhadri, S.-S. Yi, J. Phys. D: Appl. Phys. 41 (2008) 095110–095114.
[16] J. Wang, Z.Y. Zhang, M. Zhang, Q.H. Zhang, Q. Su, J. Tang, J. Alloys Compd. 488 (2009) 582–585.
[17] S. Saito, K. Wada, R. Onaka, J. Phys. Soc. Jpn. 37 (1974) 711–715.
[18] H.B. Liang, Y. Tao, Q.H. Zeng, H. He, S.B. Wang, X.Y. Hou, W. Wang, Q. Su, Mater. Res. Bull. 38 (2003) 797–805.
[19] Z.-J. Zhang, J.-L. Yuan, S. Chen, H.-H. Chen, X.-X. Yang, J.-T. Zhao, G.-B. Zhang, C.-S. Shi, Opt. Mater. 30 (2008) 1848–1853.
[20] X. Wu, Y.L. Huang, L. Shi, H.J. Seo, Mater. Chem. Phys. 116 (2009) 449–452.
[21] Y.L. Huang, W.X. Zhao, Y.G. Cao, K. Jang, H.S. Lee, E. Cho, S.-S. Yi, J. Solid State Chem. 181 (2008) 2161–2164.
[22] C.K. Jørgensen, Mol. Phys. 5 (1962) 271–277.
[23] Q. Su, in: Proceedings of the Second Conference on Rare Earth Development and Application, J. Rare Earths (1991) 765.
[24] Y.Z. Li, Y.H. Wang, Z.F. Wang, Z.Y. Zhang, J. Lumin. 130 (2010) 1225–1229.
[25] S. Cao, Y.Q. Ma, C.M. Quan, W.L. Zhu, K. Yang, W.J. Yin, G.H. Zheng, M.Z. Wu, Z.Q. Sun, J. Alloys Compd. 487 (2009) 346–350.